ELSEVIER

Tectonophysics 346 (2002) 201–222

TECTONOPHYSICS

www.elsevier.com/locate/tecto

A modern structural regime in the Paleoarchean (~3.64 Ga); Isua Greenstone Belt, southern West Greenland

Simon Hanmer [a,*], David C. Greene [b]

[a] *Continental Geoscience Division, Geological Survey of Canada, 601 Booth St., Ottawa, Ontario, Canada, K1A 0E8*
[b] *Department of Geology and Geography, Denison University, Granville, OH 43023, USA*

Received 20 April 2000; accepted 12 December 2001

Abstract

The footwall gneisses beneath the western part of the Paleoarchean (~3.8 Ga) Isua Greenstone Belt, southern West Greenland, are interpreted here in terms of a ~3.64 Ga stack of mylonitic crystalline thrust-nappes, the oldest example known on Earth. In present coordinates, the kinematic history of the thrust-nappe stack is couched in terms of initial longitudinal (strike-parallel) thrusting towards the southwest, followed by transverse thrusting to the northwest, and subsequent extensional collapse of the thickened crust toward the southeast. Diorite and tonalite that form the western margin of granitoids, structurally overlying the western part of the Isua Greenstone Belt and its footwall, contain ~3.5 Ga mafic dykes, some of which are deformed and/or truncated at fault contacts within the granitoids. Accordingly, a component of the deformation structurally above the Isua Greenstone Belt occurred after ~3.5 Ga, significantly later than the formation of the underlying mylonitic nappes, probably during the Neoarchean. The structural regime of mylonitic thrust-nappe stacking is very similar to that in modern mountain belts. It would appear that the deformational behaviour, rheological constitution and overall strength of Paleoarchean and modern continental crust were similar.

Keywords: Isua Greenstone Belt; Greenland; Paleoarchean; Thrust nappe

1. Introduction

The style of Paleoarchean tectonics is currently the subject of vigorous debate, much of which has focused on potential modern analogues for greenstone belts and their associated high-grade gneiss terranes, or the lack thereof (e.g., de Wit, 1998; Hamilton, 1998, and references therein). However, relatively few contributions to the discussion have been based on first-order structural arguments.

The mechanical behaviour of the continental crust, or indeed the lithosphere, reflects its dimensions, thermal structure and rheology, as well as the distribution and dynamic evolution of strong and weak layers (e.g., Burke et al., 1976; Ranalli and Murphy, 1987; Rutter and Brodie, 1988, 1991, 1992). Structural geological contributions to understanding the nature of Paleoarchean tectonics have generally focused on the question of dominantly vertical vs. horizontal movements within the continental crust (e.g., Park, 1997, and references therein). Some workers continue to

* Corresponding author. Fax: +1-613-943-5318.
E-mail addresses: shanmer@nrcan.gc.ca (S. Hanmer), GreeneD@cc.denison.edu (D.C. Greene).

0040-1951/02/$ - see front matter
PII: S0040-1951(02)00029-X

appeal to a hotter continental thermal regime than that of today, and identify a non-uniformitarian Archean structural regime dominated by diapirism, in some instances drawing comparisons with the Phanerozoic situation on Venus (e.g., Chardon et al., 1998; Collins et al., 1998; Hamilton, 1998; Marshak, 1999). Others favour a relatively modern structural paradigm, dominated by thrusts and nappes. However, with few exceptions (e.g., de Wit et al., 1987, 1992), such features have only been identified in Neoarchean and younger orogens (< 2.8 Ga; e.g., Bridgwater et al., 1974; Friend et al., 1996; de Wit, 1998). Komiya et al. (1999) claim to identify a ~ 3.8–3.7 Ga accretionary complex in the Isua Greenstone Belt of southern West Greenland, but their thrusting model is strongly biased by their unsupported inference of stratigraphic repetition in discontinuous units of homogeneous amphibolite and schist.

In this paper, we present the results of recent structural mapping in gneisses subjacent to the Pa-

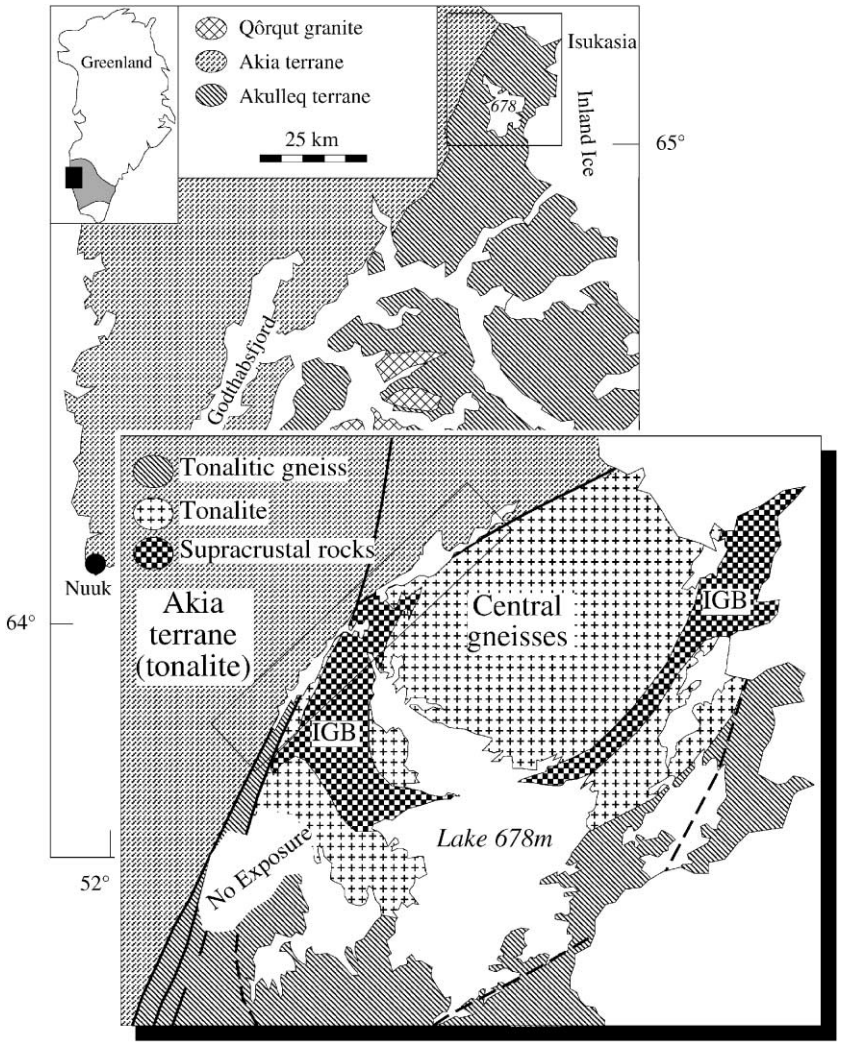

Fig. 1. Sketch map of terranes in southern West Greenland indicating the location of the Isukasia area, after Nutman et al. (1996). Inset shows sketch map of the Isukasia area highlighting the Isua Greenstone Belt (IGB). The rectangular box is the present study area (see Fig. 3). The broken line is the northern limit of strong Neoarchean deformation, taken from Nutman (1986). Note that lake names are given according to the conventions of the Greenlandic Place Names Commission.

leoarchean Isua Greenstone Belt, Isukasia, southern West Greenland (Fig. 1; e.g., Nutman, 1984, 1986; Appel et al., 1998a,b and references therein), which we interpret as a ~3.64 Ga stack of mylonitic crystalline thrust-nappes; the oldest known example of this structural style on Earth. Because they are difficult to access and have never been documented, we present detailed descriptions of the rocks, as well as the structures. We suggest that the kinematic history of the nappe stack involves initial longitudinal (strike-parallel) thrusting, followed by transverse thrusting, and subsequent extensional collapse of the thickened crust; a structural regime very similar to that in modern mountain belts.

2. Geological setting

The Archean Gneiss Complex of southern West Greenland is part of the North Atlantic or Greenland craton (Bridgwater et al., 1976). In the Godthåbsfjord area (Fig. 1), it is divided into terranes that Friend et al. (1996) suggest were amalgamated in the Neoarchean (~2.72 Ga). The Isua Greenstone Belt is located in the Akulleq terrane, adjacent to the boundary with the Akia terrane (Fig. 1). It is a narrow, arcuate belt of metamorphosed, amphibolite facies, volcanic, volcaniclastic and clastic sedimentary rocks intruded by ultramafic sills (see Nutman, 1986; Appel et al., 1998a,b; Fedo, 2000 for details). The greenstone belt is the largest intact fragment of a once extensive, supracrustal package that was intruded and dismembered by Paleoarchean (~3.80–3.62 Ga) tonalites and related granitoids of the Itsaq Gneiss Complex (e.g., Nutman et al., 1993, 1996; see also discussion in Nutman et al., 1997, 1999, and Whitehouse et al., 1999).

The arcuate Isua Greenstone Belt is flanked to the north and south by variably deformed, metamorphosed tonalitic, dioritic and granitic plutonic rocks (Fig. 1), components of the Itsaq Gneiss Complex (Nutman et al., 1993, 1996 and references therein). They have been dated by Nutman et al. (1993, 1996, 1999; U–Pb zircon SHRIMP): tonalites (~3.8–3.7 Ga), granitic sheets (~3.65 Ga), and pegmatite sheets (~3.63 Ga), interpreted as magmatic crystallisation ages in agreement with observed cross-cutting relationships (Nutman, 1984; Nutman and Bridgwater, 1986). However, elsewhere in southern West Greenland, other workers have taken issue with this interpretation, marshaling Pb–Pb, Sm–Nd and Rb–Sr data and ion-beam U–Pb zircon data, supported by cathodoluminescence imaging, to propose that the true magmatic age of the granitoids is ~3.65 Ga, and that older ages are derived from inherited zircon (see Whitehouse et al., 1999; Nutman et al., 2000, and references therein).

Few structural studies have been undertaken in the Isua Greenstone Belt and the flanking metagranitoids (James, 1976). Early work suggested that the supracrustal belt is internally symmetrical, such that the stratigraphy defines a refolded isoclinal fold whose axial trace runs along the length of the arcuate belt (Bridgwater and McGregor, 1974). Although this was challenged by Allaart (1976a), the model persisted (Nutman, 1986) until it was again called into question by Rosing et al. (1996), who showed that much of the "stratigraphy" is the product of large-scale metasomatism. Foliation in the Isua Greenstone Belt and the central gneisses is cross-cut by a polyphase swarm of Tarssartôq diabase dykes that have yielded ~3.5 Ga magmatic crystallisation ages and are correlated with the Ameralik dykes of the Godthåbsfjord area (U–Pb zircon SHRIMP; Nutman et al., 1996, 1997; White et al., 2000). The dykes are essentially pristine in the central gneisses, but are locally deformed within the Isua Greenstone Belt (Bridgwater and McGregor, 1974; Nutman, 1984). Tarssartôq dykes are also discordant to foliation in tonalitic gneisses south of the greenstone belt, where they are recrystallised as amphibolites and fewer in number (Nutman, 1986). The age of the oldest preserved metamorphism in the Isua Greenstone Belt is ~3.76 Ga (Pb–Pb ages; Moorbath et al., 1973; Frei et al., 1999) and this has been equated with the emplacement of the tonalitic plutonic precursors of the Itsaq Gneiss Complex (Boak and Dymek, 1982; Nutman et al., 1996). Boak and Dymek (1982) obtained 550 °C at 5 kbar from garnet–biotite–staurolite and muscovite–biotite–kyanite metamorphic assemblages. Despite the absence of deformation in the Tarssartôq dykes within the central gneisses, the overall arcuate geometry of the belt has been interpreted in terms of a Neoarchean dome that refolds Paleoarchean structures (e.g., Bridgwater and McGregor, 1974; Nutman, 1986).

3. Isua Greenstone Belt footwall

The western part of the Isua Greenstone Belt, and the plutonic rocks flanking it on either side, dip ~ 45–60° to the southeast such that tonalites and diorites of the central gneisses form the structural hanging wall to the supracrustal rocks. The structural footwall to the western Isua Greenstone Belt (referred to hereafter as "the footwall") is composed of tonalites, amphibolites and mafic schists that have been equated, respectively, with the plutonic rocks of the central gneisses and xenolithic rafts and smaller inclusions of mafic components of the Isua Greenstone Belt (Nutman, 1984, 1986; Nutman et al., 1984). Twenty five years ago, Allaart clearly identified and understood the potential significance of strongly banded mylonites adjacent to the greenstone belt (Fig. 2), stating that "it is tempting to suppose that the mylonitic gneisses represent relics of a major thrust zone below some of the supracrustal rocks of the Isua succession" (Allaart, 1976b, p. 71; see also figures in Gill et al., 1981; Boak and Dymek, 1982; Nutman, 1982; Appel, 1983).

We have undertaken new structural mapping of the footwall at scales between 1:10,000 and 1:20,000 (Fig. 3). Exposure is excellent, permitting direct observation and tracing of contacts, often in three-dimensions. We divide the footwall into a stack of lithologically distinct, moderately southeast dipping panels that straddle the Ataneq fault, a narrow (< 10 m), lower greenschist facies (chlorite–sericite), aphanitic ultramylonite zone of Proterozoic age (e.g., Smith and Dymek, 1983). Although the Ataneq fault extends to the Godthåbsfjord area, ~ 150 km to the southwest, only ~ 4 km of dextral separation have been documented along it (e.g., Chadwick et al., 1983; Nutman, 1986). In what follows, the individual panels are referred to by number for ease of reference; panels derived from the supracrustal rocks of the greenstone belt are indicated by the suffix "G."

3.1. Grey tonalite±mylonite panel

Because the footwall rocks east of the Ataneq fault contain identifiable protoliths, it is convenient to describe them first. In the vicinity of Lake 644, the structurally lowest panel (#1 in Fig. 3) measures ~ 4 × 0.35 km, minimum exposed strike length and approximate maximum true structural thickness, respectively. It is composed of grey tonalite with scattered rafts and xenoliths of mafic schist. The rock is medium grained, with 5 mm, rounded, plagioclase grains set in a well foliated, fine grained matrix. Locally, the grey tonalite shows strain gradients, and

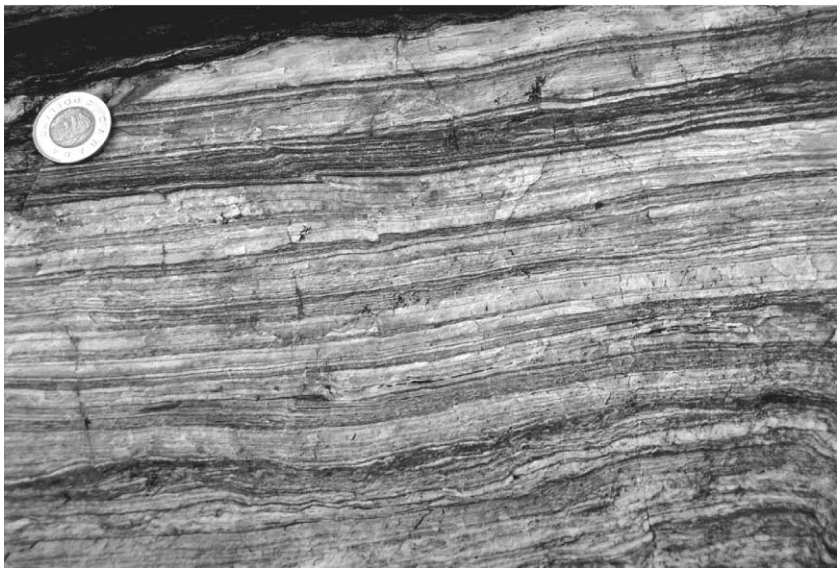

Fig. 2. Detail of ribbon tonalite mylonite from layered mylonite panel #3G (see Fig. 3). Coin, 3 cm, for scale.

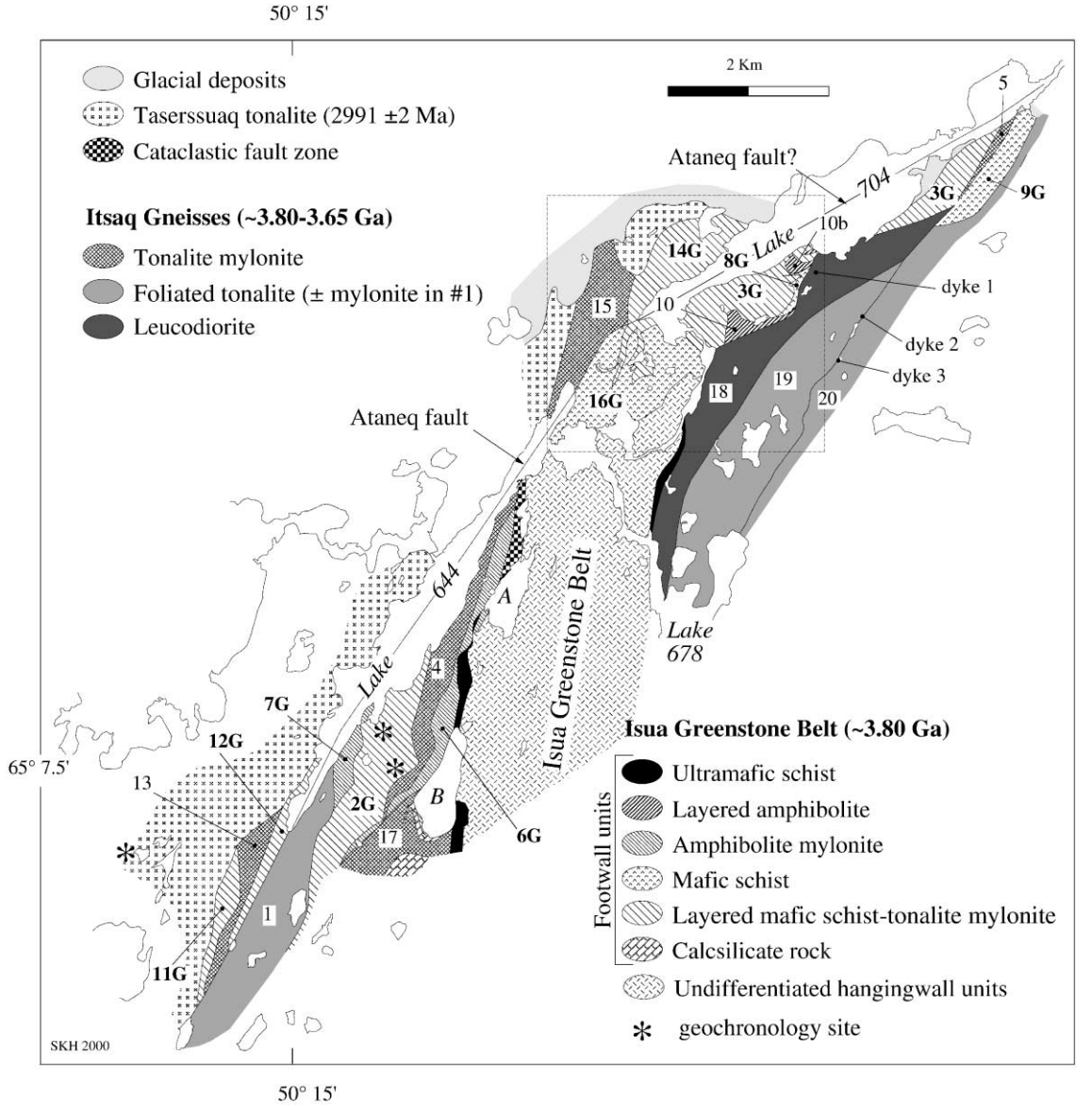

Fig. 3. Geological sketch map of northwest termination of the western part of the Isua Greenstone Belt. Mylonitic nappes in the footwall are numbered 1–15, thrust-bound granitoid panels in the western margin of the central gneisses in the hanging wall are numbered 18–20. The Isua Greenstone Belt is indicated by name, and panels derived from it are indicated by the suffix G and bold type, as in panels #16G and #17G. The location of Fig. 4 is indicated by a box. A and B are location labels for ease of reference.

mylonite with sub-millimetre size feldspar porphyroclasts is developed in anastomosing bands, between 10 cm and tens of metres thick. In many places, the mylonitic ribbon structure has been destroyed by annealing (cf. Hanmer, 1984), and only the uniformly fine grain size and the presence of porphyroclasts indicates the mylonitic nature of the rock. Thin sections show that synkinematic hydration, introduction of carbonate (carbonatisation), and postkinematic recrystallisation in the tonalitic mylonite have resulted in an annealed muscovite- and biotite-bearing quartzofeldspathic schist, with abundant disseminated carbo-

nate and clinozoisite or epidote. In places, the tonalite mylonite is cut by narrow (1–5 m) sheets of white tonalite and pegmatite, visibly injected subconcordantly with respect to the host foliation. Strongly and weakly foliated examples of both white tonalite and pegmatite cut the grey tonalitic mylonite, and mylonitic examples of both are found within non-mylonitic and mylonitic grey tonalite. Together, these observations suggest that the white tonalite and pegmatite were injected synkinematically with respect to mylonitisation.

3.2. Layered mafic schist–tonalite mylonite panel

The grey tonalite panel #1 is overlain by a similar sized panel (#2G in Fig. 3; $\sim 4 \times 0.35$ km) of dark green mafic schist intruded by thin (1–10 m) sheets of tonalite. The mafic schist is generally composed of amphibole and chlorite and is strongly foliated. However, parts are less phyllitic, more feldspathic, and less schistose, although they still present a very strongly developed planar anisotropy. These rocks were intruded by subconcordant sheets of grey and white tonalites, as well as pegmatite. Locally, subconcordant sheets of white tonalite and pegmatite pervasively intruded the grey tonalite and result in a well developed compositional layering in granitoid units 10–50 m thick. The distribution of the tonalite sheets is uniform throughout the panel and unrelated to proximity of the panel boundaries.

At the outcrop scale, the tonalitic components of this panel are pervasively mylonitised. Both grey and white tonalites commonly contain apparent ribbon fabrics, and the grey tonalite is commonly charged with fine (1–2 mm) plagioclase porphyroclasts. However, in detail, less strongly deformed white tonalite sheets locally cut grey tonalite mylonite, suggesting that the former was injected synkinematically with respect to mylonitisation. In thin section, the tonalite mylonites are hydrated and carbonatised quartzofeldspathic schists, similar to those in the grey tonalite panel #1, with the grey and white tonalite components differing principally in biotite and sericite (after plagioclase) content. Plagioclase porphyroclasts, where present, show fracturing, kinking and mortar textures indicative of mixed brittle and crystal plastic behaviour (e.g., Hanmer, 1982; Pryer, 1993), but the abundance of white mica and epidote minerals highlights the important role played by chemical change during deformation (e.g., Fitzgerald and Stunitz, 1993; O'Hara, 1994). Polycrystalline quartz ribbons wrap around feldspar porphyroclasts, and show a marked tendency to vary in thickness and anastomose. Mackinnon et al. (1997) interpret similar features as fracture controlled quartz veinlets introduced into the deforming rock. A strain gradient in the lowermost ~ 25 m of panel #2G is well exposed at the shore of lake 644. There, the mylonite is more planar and distinctly flaggy, and transposition is so penetrative that few tonalite sheets preserve evidence of their intrusive nature.

Very similar rocks form a panel (#3G in Fig. 3; 4.5 km minimum strike-length) separated into two parts by the eastern shore of Lake 704. Geometrically, the northern part of panel #3G is identical to panel #2. However, the southern part of panel #3G is characterised by gently doubly plunging, east–northeast trending, 100–200 m wavelength, open, upright, horizontal folds that deform the mylonite fabric (Fig. 4). The folds verge to the north–northwest, with a shallowly south–southeast dipping enveloping surface, and an axial plane that dips in the range 45–70° in the same direction.

3.3. Tonalite mylonite panel

East of Lake 644, the layered mylonite panel #2 is overlain by a thinner panel (#4 in Fig. 3; $\sim 4.5 \times 0.15$ km) of homogeneous, light grey tonalite with few inclusions. The northern half of the panel is extremely fine grained and non-fissile. In places, it has a sugary texture and the appearance of an undeformed aplitic rock. However, because it passes along strike into well developed ribbon mylonite in the southern half of the panel, we suggest that the sugary texture is due to annealing. Contacts with adjacent panels are abrupt. While it may be related to the intrusive tonalites in the underlying layered mylonite panel #2G, it contains no inclusions in the vicinity of the contact. Adjacent to the upper contact, inclusions of mafic schist in the tonalite are quite distinct from the mafic rocks of the overlying amphibolite panel (#6G; see below). We suggest that both contacts are abrupt faults. A narrow panel (#5 in Fig. 3; 1.0×0.07 km) of similar looking tonalite ribbon mylonite overlies the layered mylonite panel #3G east of Lake 704.

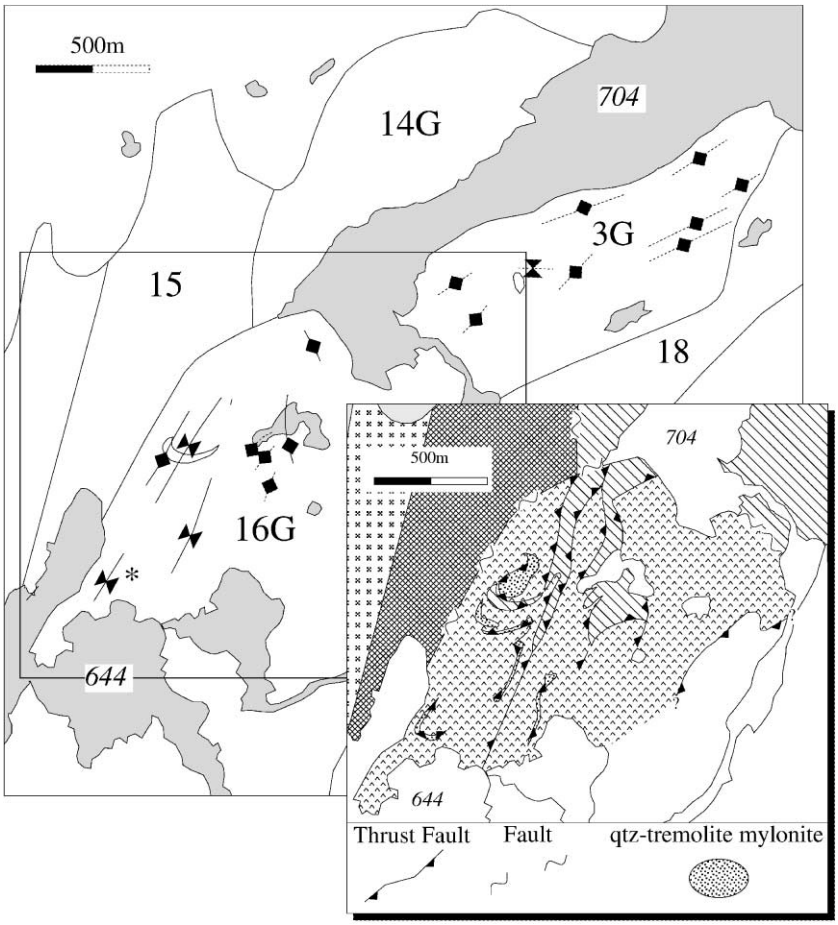

Fig. 4. Sketch of the area between Lakes 644 and 704 to illustrate the distribution of axial traces of open, upright, horizontal folds that deform the mylonitic foliation and intrafolial sheath folds. The fold in the southwest marked by an asterisk is illustrated in Fig. 5. Outlines of numbered mylonitic panels are shown; see Fig. 3 for geology. Inset is a detail of the geology of panel #16G to illustrate the disposition of quartz–tremolite mylonites (grey shading). Other lithologies are as in Fig. 3.

3.4. Amphibolite mylonite panels

Panels of compositionally homogeneous, dark green to black amphibolite occur at two structural levels east of Lake 644 (#6G and #7G in Fig. 3; $5 \times 0.05–0.35$ km and 1.5×0.25 km, respectively). Both amphibolite panels are characterised by a uniformly fine grain size and, where visible, a strongly developed, planar, compositional lamination. The lowermost 20 m of panel #6G are intruded by thin (< 1 m) white pegmatite sheets that, for the most part, are mildly foliated. However, in a strain gradient at the southern end of the panel, the pegmatites are penetratively mylonitised along with the amphibolite, which itself looks no different to the mafic rock throughout the rest of the panel. We suggest that the strong lamination in both amphibolite panels is a mylonitic foliation. The ductile strain gradient was locally reworked by later brittle faulting, resulting in limited post-pegmatite breccia zones 1–10 m thick.

Panels of mafic schist (#8G and #9G in Fig. 3; 1.8 and 0.75 km exposed strike length, respectively), indistinguishable from that in the layered mylonite, but with few tonalite sheets, occur east of Lake 704. The smaller of the two, panel #8G, is overlain by a panel (#10 in Fig. 3; 1.0×0.15 km) of thickly banded

amphibolite, compositionally layered on a 0.5–1.0-m scale, which also occurs as a synformal outlier (panel #10b) near the shore of the lake. Much of the compositional layering has been effaced by deformation-related processes. However, where well preserved, it is highlighted by variation in the proportion of 2 cm scapolite porphyroblasts. The basal 2 m of the panel are locally riddled with highly deformed, attenuated quartz veins. Where the veins are strongly boudined, the resulting tectonite has the aspect of a porphyroclastic gneiss (e.g., Hanmer, 1988a).

3.5. Panels west of Ataneq fault

West of Lake 644, two layered mylonite panels (#11G and #12G in Fig. 3), separated by a panel of tonalite mylonite (#13 in Fig. 3), are lithologically and dimensionally (up to 5×0.2 km) indistinguishable from panels #2G and #3G described above from the east side of the Ataneq fault. They were intruded by the ~ 3.0 Ga Taserssuaq tonalite complex (Hanmer et al., submitted for publication; see also Chadwick et al., 1983). West of Lake 704, two panels of layered mylonite and tonalite mylonite (#14G and #15, respectively, in Fig. 3) are juxtaposed across a narrow zone of cataclasis and minor mylonite, similar to rocks in the Ataneq fault zone, of which this could represent a minor splay. Both panels are intruded by the Taserssuaq tonalite, and the fault splay does not ap pear to significantly offset the intrusive contact.

4. Isua Greenstone Belt

4.1. Mafic schist

The northwestern limit of the Isua Greenstone Belt is exposed between lakes 644 and 704, where it is truncated by the Ataneq fault (see also Bridgwater and McGregor, 1974; Nutman, 1986). The supracrustal rocks are represented by homogeneous mafic schist (panel #16G in Fig. 3), which at least locally contains well preserved mafic pillows (see also Appel et al., 1998a,b). The mafic schist is intercalated with thin (50 m) panels of layered mafic schist–tonalite mylonite, identical to that described for the footwall (panels #2G and #3G in Fig. 3). The mafic schist also contains thin, discontinuous panels of laminated quartz–tremolite ± sulphide mylonite (Fig. 4). The siliceous mylonites are generally only a few metres thick, although in places, internal isoclinal folding results in thicknesses

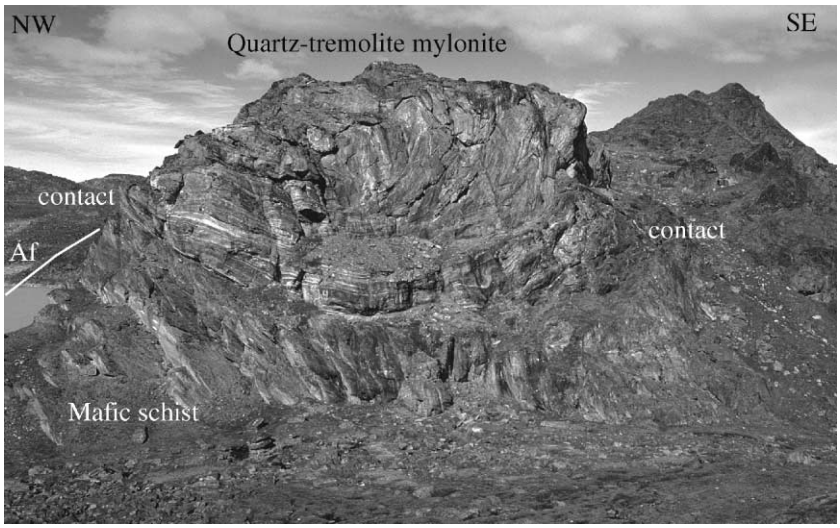

Fig. 5. View looking north of quartz–tremolite mylonite (above contact), internally folded and thickened by intrafolial, isoclinal folding, which occupies an open, upright, horizontal, synformal closure, underlain by mafic schist (below contact), in panel #16G. Note that foliation in the mafic schist is concordant to the lithological contact. The topographic expression of the Ataneq fault (Af) at the north end of Lake 644 is visible to the far left. Outcrop face ~ 50 m high. See Fig. 4 for location.

of up to 30 m (Fig. 5). The initial dimensions of these units are compatible with an origin as siliceous dolomites or dolomitic cherts. However, in a rare low strain window, abundant schistose fragments of mafic schist are markedly misoriented within a non-foliated quartz sheet that also contains irregular masses of carbonate. The whole assemblage is transformed to laminated, schistose, quartz–tremolite mylonite along the margin of the sheet. Another example is compositionally zoned, with carbonate symmetrically concentrated along the sheet margins. These observations suggest that the quartz–tremolite mylonites were derived from quartz–carbonate veins.

The interlayered assemblage of mafic schist, quartz–tremolite and layered mylonite is deformed by gently doubly plunging, east–northeast trending, open, upright, horizontal folds (Fig. 5), with 100–200 m wavelengths, similar to those described for the footwall rocks in panel #3G, immediately to the northeast. Here, these folds are well defined by relatively continuous horizons of quartz–tremolite mylonite. Again, the folds verge to the north–northwest, with a shallowly south–southeast dipping enveloping surface and moderate to steeply south–southeast dipping axial planes.

4.2. Ultramafic schist

East of Lake 644, the supracrustal rocks of the Isua Greenstone Belt are separated from the footwall panels described above by a steeply dipping, fine grained, dark green to grey, ultramafic schist composed of a talc matrix with dispersed grains of carbonate and actinolite. The ultramafic schist is up to 150 m thick in the south, but it narrows to ~ 10 m in the north, where it occurs as discontinuous lenses. North of the small lake marked A (see Fig. 3), it is succeeded along strike by a diffuse cataclastic fault zone, up to 180 m thick, which contains small, discontinuous lenses of ultramafic schist. To the south, it extends into the core of the Isua Greenstone Belt, and across Lake 678 (Nutman, 1986; J. Myers, unpublished data, 1999).

4.3. Tonalite mylonite and calcsilicate rocks

South of the small lake marked B (see Fig. 3), the ultramafic schist and the mylonitic panels of the footwall are separated by a ~ 1.4 km thick tract of compositionally homogeneous quartzofeldspathic schist and calcsilicate rocks, with subordinate amphibolite and ultramafic schist (#17 in Fig. 3). This map unit has long been treated as part of the supracrustal belt stratigraphy (e.g., Nutman, 1986). The quartzofeldspathic schist is a grey to light brown, intensely foliated, steeply dipping, fine grained S > L to L>S tectonite, with a strong, steeply plunging extension lineation. Locally, vivid green silicious units, up to several metres thick, contain fuchsitic mica (Dymek et al., 1983). In thin section, a fine grained (50 μm) quartzofeldspathic matrix is pinned by abundant, disseminated, fine grained biotite and white mica. What appeared macroscopically to be ribbons are either single-chain polycrystalline quartz veins, or very straight, narrow seams of biotite and muscovite. Abundant carbonate and clinozoisite are disseminated throughout the matrix, and are likely responsible for a locally pronounced vuggy weathering. Microscopically, the quartzofeldspathic schist bears a strong resemblance to the hydrated and carbonatised tonalitic mylonites of the footwall, described above. However, both its mylonitic fabric and extension lineation are more strongly developed than in the footwall rocks.

The calcsilicate material is a soft, buff, calcareous, feldspathic rock, associated with fuchsitic siliceous layers from 1 cm to several metres thick. This association occurs in two principal, map-scale bodies, separated from the enclosing quartzofeldspathic schist by contacts that vary from sharp to progressive. In thin section, it comprises a homogeneous, medium to fine grained, polycrystalline plagioclase–carbonate matrix with loosely aligned, disseminated laths of biotite and white mica. The ultramafic schist is light tan coloured and occurs as discontinuous bodies up to 5 m thick by several tens of metres long. Microscopically, it comprises a talc matrix with disseminated, equigranular, equant grains of carbonate.

The map-scale geometry of these units describes a steeply plunging Z fold, with kilometre-scale wavelength and amplitude, that deforms the mylonitic foliation, but is coaxial with the mylonitic extension lineation. The mylonitic fabric symmetry varies systematically from S>L tectonite on the fold limbs, to a pronounced L>S tectonite in the fold core. This suggests that the mylonitic fabric was still evolving

while the Z fold developed, but after the main mylonite-forming episode.

5. Central gneisses

The foliated tonalitic, dioritic and granitic rocks of the central gneisses (Fig. 1), and the mafic dyke swarm that cuts them, have been described in detail elsewhere (e.g., Nutman and Bridgwater, 1986 and references therein). Much of the granitoid is represented by foliated tonalite and leucodiorite southeast of Lake 704 (Fig. 3). For the most part, foliations dip moderately to the southeast and appear to be parallel to the principal map-scale lithological contacts, such that the plutonic rocks structurally overlie the western part of the Isua Greenstone Belt and its footwall. The lowermost unit is a medium grained, equigranular, grey-green, biotite–hornblende leucodiorite (#18 in Fig. 3). It is poorly foliated, but contains rare xenoliths of strongly foliated mafic schist, indicating an intrusive relationship to adjacent rocks. It is abruptly overlain by a dark to medium grey, equigranular, variably foliated, biotite tonalite (#19 in Fig. 3), itself in sharp contact with, and included as xenoliths and rafts within, an overlying coarse grained, light grey to white, moderately foliated, biotite tonalite (#20 in Fig. 3). All three plutonic map units are cut by large, locally very coarsely (up to 5 cm) plagioclase–phyric, diabase dykes, up to 50 m thick. The latter are part of the ~3.5 Ga Tarssartôq dyke swarm (Nutman et al., 1996, 1997; White et al., 2000).

The lowermost 200 m of the leucodiorite (panel #18 in Fig. 3) are strongly altered and well foliated, although the macroscopic expression of the fabric has been attenuated by recrystallisation and annealing. In thin section, plagioclase is extensively replaced by clinozoisite, and hornblende is altered to biotite and then to chlorite. A 10-m-thick, branching, plagioclase–phyric, Tarssartôq dyke (dyke 1 in Fig. 3) is concordant to, and penetratively affected by the leucodiorite foliation.

Similar Tarssartôq dykes have been previously mapped (Nutman, 1986) in the darker and lighter grey tonalite units in panels #19 and 20, respectively. Several examples occur at the abrupt contact between the two panels. The basal 1–2 m of a 10-m-thick ophitic dyke (dyke 2 in Fig. 3) that lies parallel to the contact were converted to chlorite schist and injected by 25–50 cm thick tonalite veins that are now ribbon mylonite. Along strike to the southwest, a 10–20-m-thick, plagioclase–phyric dyke (dyke 3 in Fig. 3), that makes an high angle (~70°) with the contact between the two panels, is abruptly truncated at the contact itself. A second similar dyke truncation occurs at the same contact, several hundred metres along strike to the southwest. These observations indicate that some of the contacts within and bounding the central gneisses are tectonic with localised foliation development, and that deformation at the contacts postdates the ~3.5 Ga Tarssartôq dykes.

6. Structure and kinematics

The map-scale geometry of the map-unit boundaries (Fig. 3) and the concordant, layer-parallel, mylonitic foliation in the study area is relatively simple; moderate (~45–60°) dips to the east and southeast, with local, map-scale, upright, horizontal, open to moderate folds that deform the foliation (see Figs. 4 and 5). In contrast, the orientations of extension lineations within the mylonitic foliation (Fig. 6), and outcrop and smaller scale intrafolial fold axes that deform the foliation, is more complex. The extension lineation is mostly oriented northwest–southeast, transverse to the structural grain, with a subordinate longitudinal population oriented northeast–southwest, a pattern that is readily discerned between lakes 644 and B (Fig. 6). The fold axis pattern is best developed in the layered mylonite panels, where the multilayer rheology favours folding at all scales, as well as in the laminated quartz–tremolite mylonites enclosed in mafic schist. In a given outcrop, the intrafolial folds bear a systematic relationship to the local finite extension direction, such that fold axes make lower angles with the extension lineation as the fold profile tightens. In some cases, this relationship can be followed around the curved axis of a single fold at a scale varying from 25 cm to 5 m. The curved fold axes are bisected by the local finite extension direction, where present, and are clearly sheath folds (Fig. 7; Cobbold and Quinquis, 1980; Bell and Hammond, 1984). The folds commonly form lenticular packages that are enclosed by mylonite derived by transposition of the folded fabric (Fig. 8). This style of deformation, whereby folded mylonite

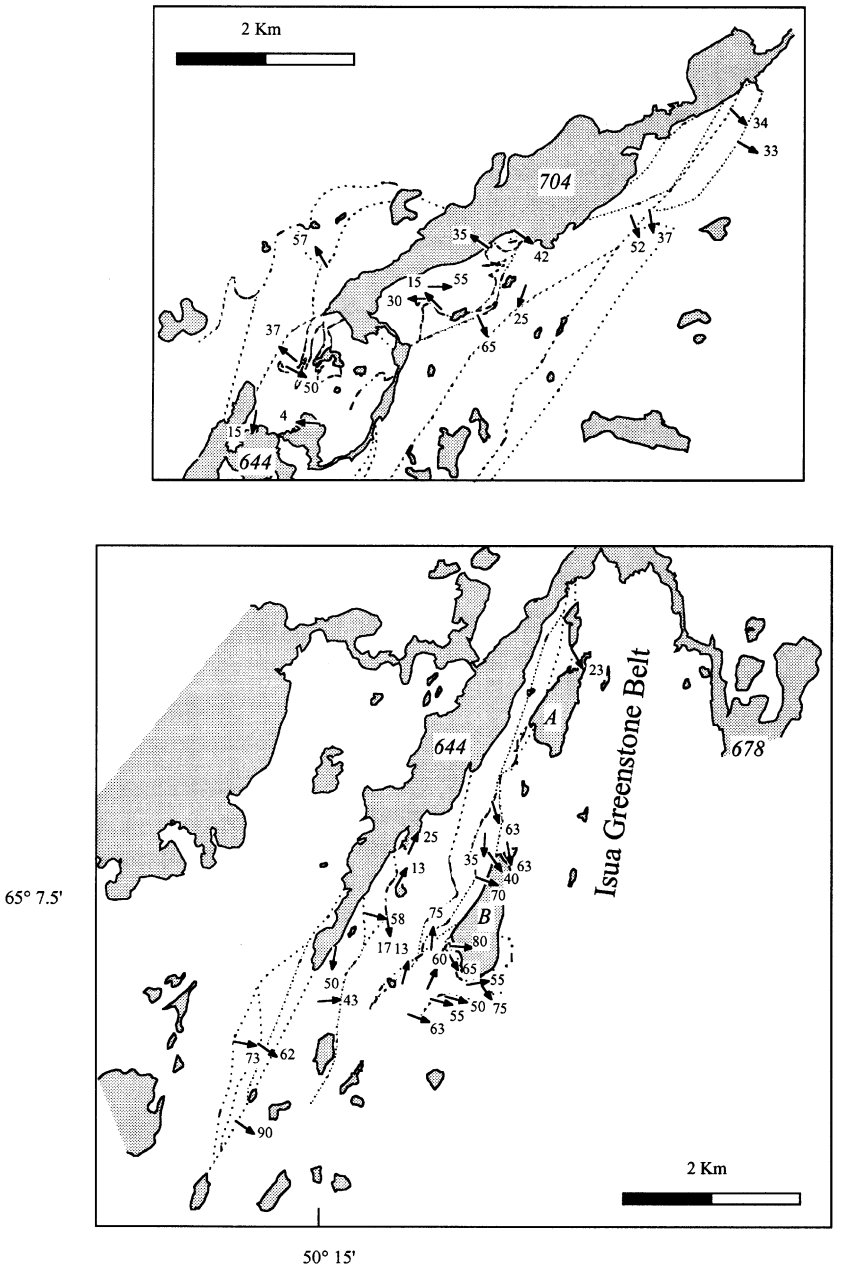

Fig. 6. Detailed maps of extension lineation orientations. The boundaries of the mylonitic panels are indicated by broken lines; see Fig. 3 for geology.

was transposed to form new, anastomosing to planar mylonite zones, is characteristic of the layered mylonite panels #2G and #3G at all scales up to 50–100 m in true thickness (see Fig. 9). From this, we conclude that the intrafolial folds were coeval with at least the later stages of mylonitisation *in any given location*.

Shear sense indicators, such as asymmetrical extensional shear bands, C/S fabrics, back-rotated pull-

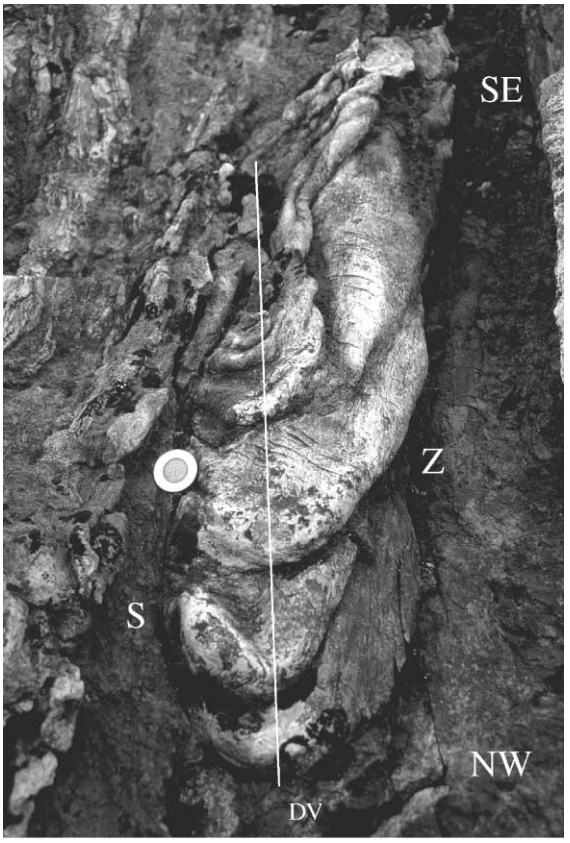

Fig. 7. A nest of sheath folds, exposed in three dimensions, developed in a tonalite sheet within mafic schist in layered mylonite in panel #3G. The displacement vector (DV) responsible for the development of these folds bisects the strongly curved fold axes along the line of sight of the observer. The sheath fold segments vary in vergence on either side of the displacement vector (S and Z). Shear sense here is top-toward-observer. This outcrop represents station 20 in Fig. 10. Coin, 3 cm, for scale.

aparts or foliation fish (e.g., Hanmer and Passchier, 1991), are sparse in the mylonitic rocks in the Isua Greenstone Belt footwall. However, the intrafolial fold orientation distribution pattern can be used for kinematic analysis. Hansen (1971) has demonstrated that by tracking the relationship between fold asymmetry and the sense of rotation of the fold axis with progressive deformation, it is possible to determine the slip direction and the shear sense of the flow that generated the folds (e.g., Figs. 7 and 9). This is equivalent to observing the fold asymmetry of developing sheath folds (Cobbold and Quinquis, 1980). In a monoclinic shear zone that has not extended significantly along the vorticity vector, the displacement vector is likely to lie close to the finite extension lineation at relatively high magnitudes of strain (see Passchier et al., 1997; Passchier, 1998). However, in other cases, the angular relationship between displacement and extension lineation may be more complex, especially in triclinic shear zones (see Lin et al., 1998). In any event, extension lineations are only patchily preserved in much of the footwall (Fig. 6) and are commonly absent where the folds are best developed. Accordingly, it is necessary to formally derive the displacement vector directly from the fold population. Application of this method can be complicated by rotation of the shear plane, either during sheath fold amplification or due to later folding, that could lead to apparent reversal of shear sense (e.g., Alsop and Holdsworth, 1999). However, in the footwall to the western part of the Isua Greenstone Belt, megascopic (larger than outcrop scale) intrafolial or recumbent folds are absent, and the ~ 200 m wavelength folds that deform the sheath folds are open, upright and horizontal.

Twenty-eight stations were selected for detailed measurement, where the outcrop-scale enveloping surface to the folds had not been disturbed by later events *within* the station, and the results are presented as annotated stereoplots (Fig. 10; see Fig. 11 for station locations). The kinematic analysis was performed by initially finding the best-fit great circle to the intrafolial fold axis point data using *R*. Almendinger's Stereonet programme. The displacement direction is the radius of the plot that best divides the pont data into two-fold symmetry populations, and the shear sense is determined from inspection of the distribution of fold symmetries on either side of the displacement vector. The present orientation of the best-fit great circle may be disturbed by rigid body tilting associated with younger events at a scale greater than the station, e.g., upright, horizontal folding or faulting, hence, the present dip of the great circle in a given plot is not considered to be kinematically significant with respect to the mylonitisation events. A direct confirmation of the validity of the method is afforded by station 20 (Fig. 10), where all 20 points were measured on a nest of stacked sheath folds exposed in three dimensions, with an amplitude of ~ 1 m (Fig. 7).

Most of the stereoplots show some deviation from the ideal, i.e., the distribution of fold symmetries is

Fig. 8. Small-scale example of the progressive development of planar mylonite zones by the transposition of intrafolial folds of earlier formed mylonite in the layered mylonite panel #2G. The asymmetry of the folds between the two bounding planar zones is compatible with transverse thrust kinematics. In other outcrops, at a larger scale, intrafolial folds associated with transverse extensional kinematics deform the equivalents of the planar mylonite zones shown here; see Figs. 9 and 12. Hammer for scale.

not mutually exclusive across the displacement vector. Non-ideal stereoplots may reflect (i) initial deviation from a simple, planar configuration in the pre-fold mylonite foliation surface that can either influence the symmetry of a given fold as it develops from the initial perturbation (e.g., Anthony and Wickham, 1978; Manz and Wickham, 1978), or control the plunge of the fold (e.g., Ghosh et al., 1993), (ii) superimposed displacement vectors, and/or (iii) the presence of small-scale, inverted, intrafolial fold

Fig. 9. A large-scale example of the development of intrafolial sheath folding in the layered mylonite of panel #2G. In the foreground, mafic schist and tonalite mylonite are deformed by recumbent sheath folds. The intrafolial fold axis is perpendicular to the outcrop face in the centre (a) and to the left, but turns progressively to parallel to the outcrop face at the right (b). Hansen analysis of this outcrop (station 4 in Fig. 10) indicates west directed transverse thrusting. Note also the thrust-nappe style of the folds with extreme lower limb attenuation (c). The outcrop defining the skyline (above d–d′), approximately 300 m behind the foreground rocks, is a mylonite zone dipping gently to the east (right). This outcrop structurally overlies the foreground rocks, and the intrafolial folds in the latter were progressively transposed to form the mylonites of the former. A continuous train of mesoscopic, curvilinear folds of Z asymmetry (not visible at this resolution) forms a cascade indicative of top-to-east extensional shearing; see also station 3 in Fig. 10. Geological hammer (left of centre) for scale.

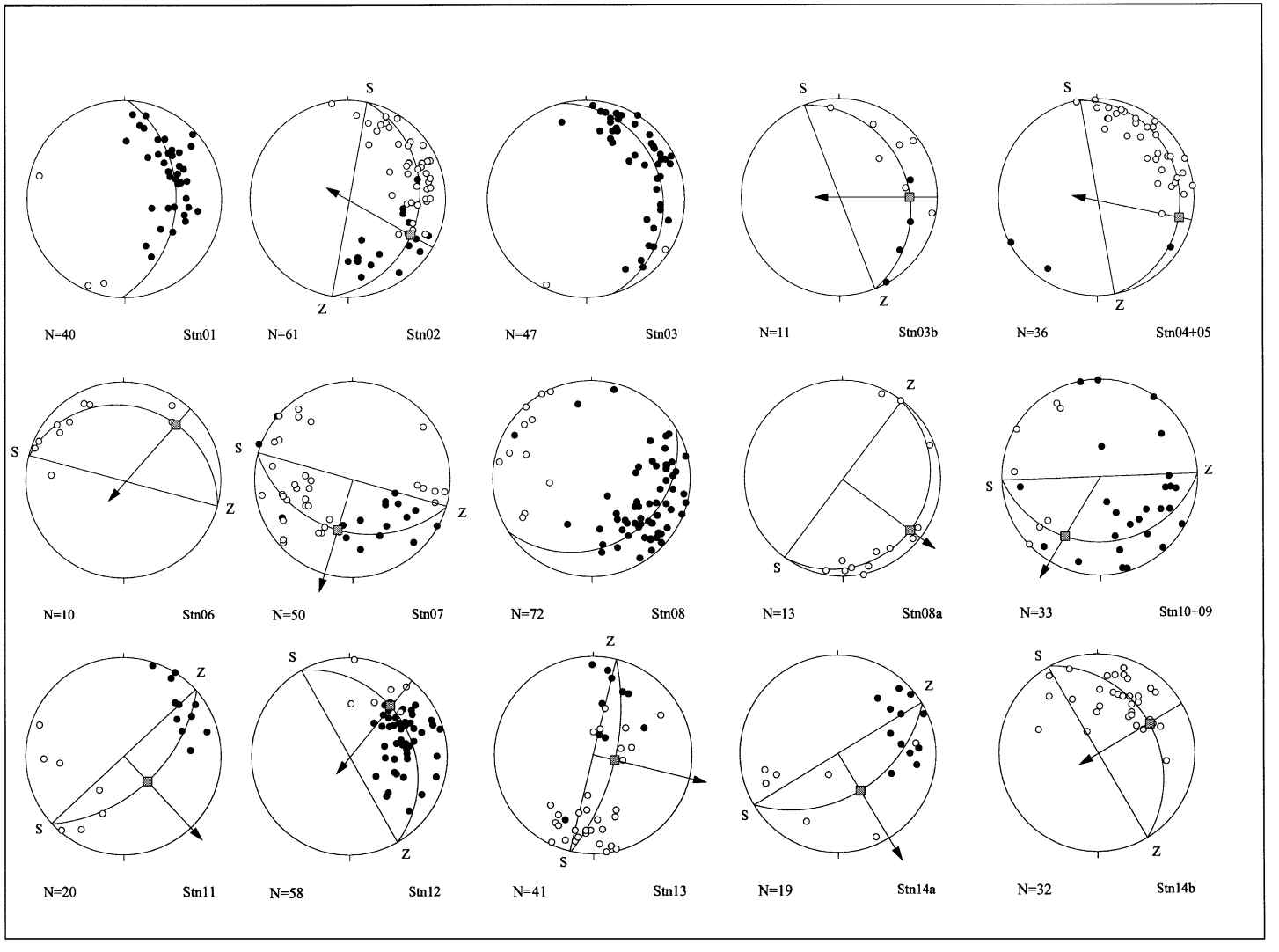

Fig. 10. Kinematic analysis of non-coaxial intrafolial sheath folds. Method is described in the text. However, an additional minor rotation was applied to the displacement vectors for stations 4 + 5 and 21 (15° clockwise and counterclockwise, respectively) to enhance the fold symmetry distribution on either side of the vector. Symbol key is given at lower right. *N* is the number of measurements. Station numbers are geographically located in Fig. 11.

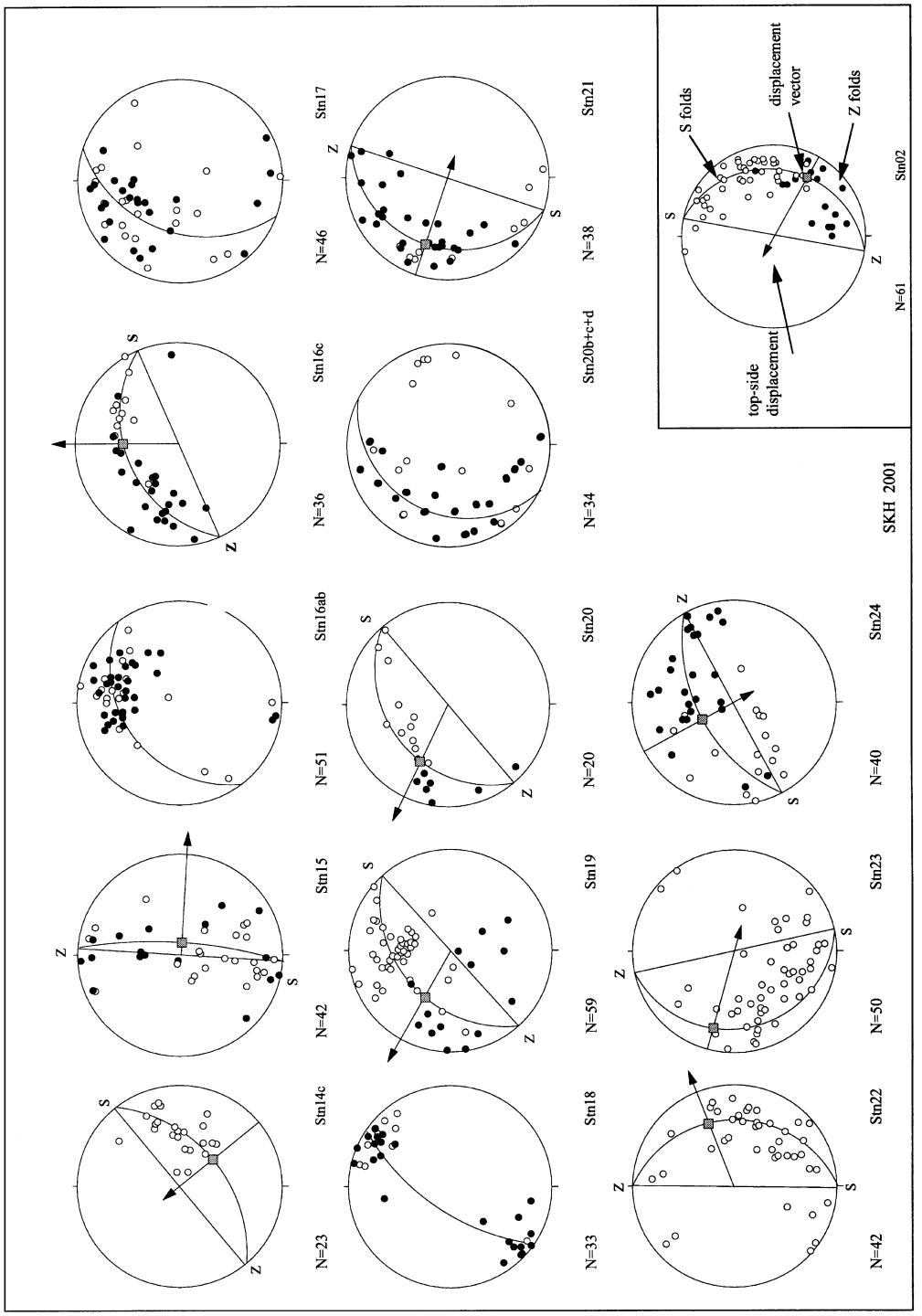

Fig. 10 (*continued*).

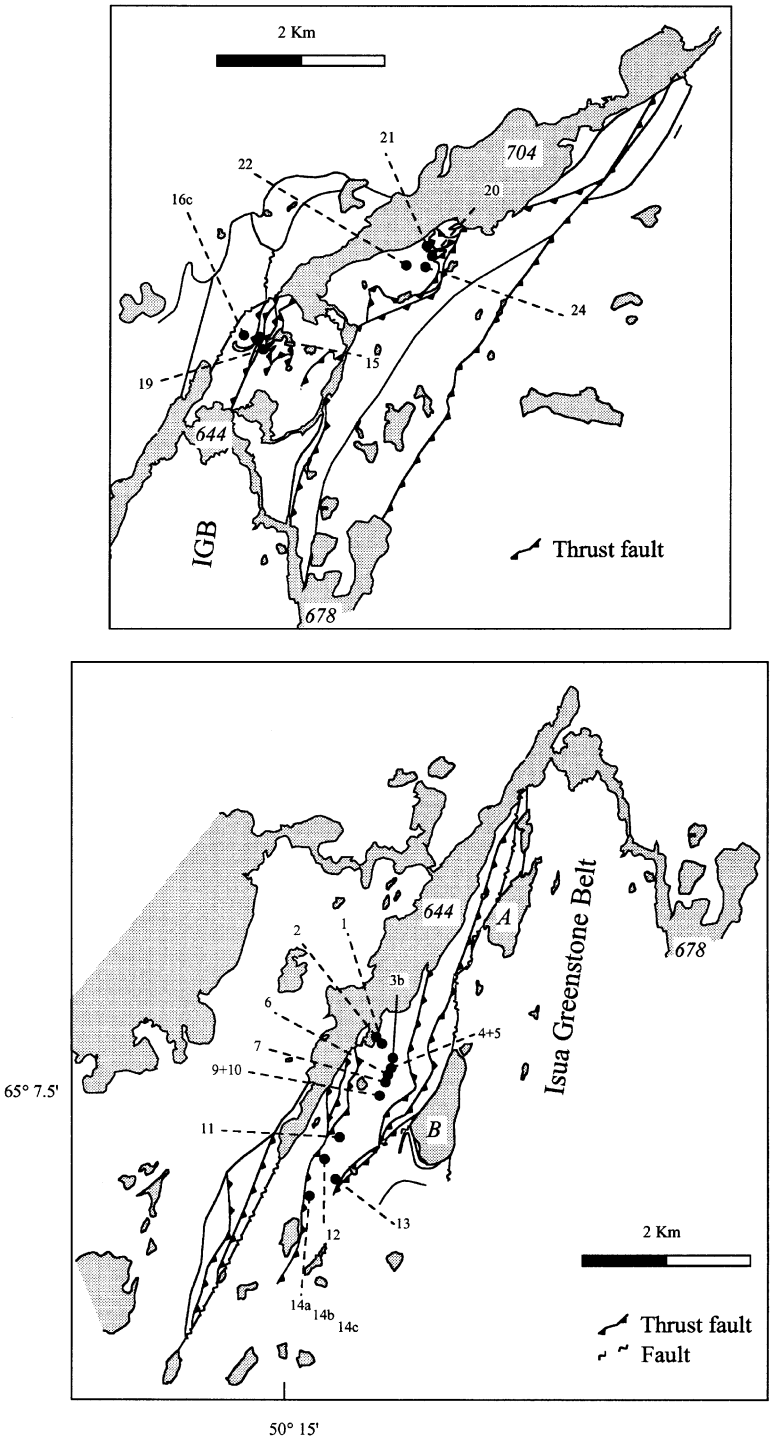

Fig. 11. Sketch map indicating the pattern of thrust-nappe boundaries and faults. Numbers refer to station locations in Fig. 10.

limbs. However, in most cases, either there is a clear predominance of a one-fold symmetry on each side of the displacement vector (e.g., stations 2, 3b, 7, 11, 13, 14a, 15, 16c, 19, 20, 21 and 24 in Fig. 10), or folds of a given symmetry are confined to one quadrant of the plot (e.g., stations 4 + 5, 6, 8a, 14b, 14c, 22 and 23).

Throughout the study area, deduced displacement vectors and shear sense in the layered mylonite panels and the quartz–tremolite mylonite fall into three groups: (i) longitudinal top-side–southwest, (ii) transverse top-side–northwest (see also Fig. 9), and (iii) transverse top-side–southeast (see also Fig. 12). Where present, scarce independent shear sense indicators (see above) invariably confirmed this deduction. Expressed in terms of the present-day southeast regional dip, these vectors correspond to longitudinal strike-slip movement (stations 6, 7, 9 + 10, 12 and 14b in Fig. 10), transverse thrusting (stations 2, 3b, 4 + 5, 14c, 16c, 19 and 20), and transverse extensional shear (stations 8a, 11, 13, 14a, 15, 21, 22, 23 and 24), all along shallowly dipping shear planes. Other stations yield equivocal results (stations 1, 3, 8, 16, 17, 18 and 20bcd; locations omitted in Fig. 12 for clarity). Where stations are juxtaposed, and outcrop is continuous, it is possible to demonstrate by direct observation that the transverse extensional displacement vectors were superposed on planar fabrics derived by the total transposition of folded mylonites characterised by earlier transverse thrusting vectors (stations 1 and 2, and 3b in Fig. 11; see also Fig. 9). This is an important observation because it demonstrates that the shear sense reversal is real and not the result of megascopic fold limb inversion (cf. Alsop and Holdsworth, 1999). In other cases, the timing relationship cannot be directly observed (stations 14a and 14c, 15 and 19, 20 and 24), but the stations are closely juxtaposed, all fabric elements are mutually parallel, and there is no evidence for megascopic intrafolial or recumbent fold limb inversion.

The longitudinal strike-slip vectors were all measured in the core of the layered mylonite panel east of Lake 644 (Fig. 11). Although their relative timing with respect to the transverse displacement vectors was nowhere directly observed, their preservation in the centre of the thickest layered mylonite panel suggests that early strike-slip mylonites were reworked by transverse contractional mylonitisation along the panel margins, which itself generated transposition zones that were exploited during later extensional shear.

7. Timing of deformation

Nutman (1986) identified a boundary south of the Isua Greenstone Belt that represents the northern limit of intense Neoarchean (~ 2.82–2.72 Ga; e.g., Nutman et al., 1996; Friend et al., 1996) regional deformation and metamorphism (see inset in Fig. 1). In later publications (Nutman et al., 1999), this limit was extended to the northwest, apparently placing the mylonites of the present study area on the Neoarchean

Fig. 12. Train of curvilinear Z folds in quartz–tremolite mylonite in panel #16G indicative of top-to-east (right) extensional shearing along a gently east dipping plane. A horizon of talc schist (light grey) occurs beneath the mylonite to the left (a). Field of view ~ 50 m wide.

side of the boundary. However, as noted above, the mylonitic panels of the footwall were intruded by the Taserssuaq tonalite complex, a large plutonic body that occupies the eastern third of the Akia terrane (e.g., Garde, 1997). It is a largely homogeneous body, extending from the Inland Ice to the Godthåbsfjord area, where it intrudes rock units on its eastern margin (Chadwick et al., 1983). In our study area, the Taserssuaq tonalite is an equigranular, medium grained (~ 5 mm), leucocratic tonalite with a weakly developed magmatic foliation. It intrudes and contains misoriented rafts, 50 m long by 10 m thick, of open folded, layered mylonite, demonstrating that the Taserssuaq tonalite was emplaced after mylonitisation, and probably after deformation of the mylonite and its intrafolial sheath folds by the late upright, horizontal folding (Fig. 4). A sample taken ~ 1 km west of the mylonites (Fig. 3 for location), has yielded a U–Pb zircon magmatic crystallisation age of 2991 ± 2 Ma (Hanmer et al., submitted for publication), confirming the 2982 ± 7 Ma age obtained from a site 25 km further west (e.g., Garde et al., 1986; Garde, 1997). This result provides a minimum age for mylonitisation west of the Ataneq fault.

In addition to the Taserssuaq tonalite, deformed tonalite and pegmatite sheets from within the mylonitic footwall panels have been dated by the U–Pb zircon SHRIMP technique (Hanmer et al., submitted for publication). A tonalite sheet that provides a maximum age for mylonitisation yielded a magmatic crystallisation age of $\sim 3640 \pm 3$ Ma. A cross-cutting, non-foliated pegmatite sheet that provides a minimum age for intense deformation and mylonitisation east of the Ataneq fault was dated at 2948 ± 8 Ma, compatible with the result derived from the Taserssuaq tonalite on the west side of the fault. Zircon rims and overgrowths dated at ~ 2950 and ~ 2680 Ma in both samples are broadly comparable to the ~ 2980 Ma event in the Akia terrane (Nutman et al., 1989), and the ~ 2720 Ma granitoid sheets common to the Akulleq, Akia and Tasiusarsuaq terranes (Friend et al., 1996). Finally, we note that mylonites with Paleoarchean, synkinematic tonalite sheets, similar to those described here, albeit much thinner (~ 10 m), are cross-cut by pristine ~ 3.5 Ga Tarssartôq dykes at the contact between the central gneisses and the Isua Greenstone Belt, east of Lake 678 (Crowley et al., 2000; White et al., 2000).

Extensive SHRIMP geochronology demonstrates that tectonothermal and magmatic events throughout the Akulleq terrane occurred during two extended periods: ~ 3870–3500 Ma and ~ 2840–2700 Ma (e.g., Nutman et al., 1996, 2000; Friend et al., 1996; see also Frei et al., 1999). Although the history of the Paleoarchean period is the subject of lively debate (e.g., Whitehouse et al., 1999; Nutman et al., 2000 and references therein), there is general agreement that a major regional tectonothermal event occurred at ~ 3650 Ma, manifested as granulite facies metamorphism in the vicinity of Godthåbsfjord, and amphibolite facies metamorphism and the intrusion of granitoids at higher crustal levels in the Isukasia area (e.g., Nutman et al., 1996; see also Crowley et al., 2000). No regional tectonothermal event has so far been detected in the interval 3500–3000 Ma (Nutman et al., 1989, 1996, 2000). Our geochronological data (Hanmer et al., submitted for publication) fit well with the existing regional database and indicate that the mylonitic panels in the footwall to the western part of the Isua Greenstone Belt formed during the Paleoarchean at ~ 3640 Ma.

Isotopic studies in the Isua Greenstone Belt have detected a Neoarchean metamorphic disturbance at ~ 2.85 Ga (Gruau et al., 1996; Frei et al., 1999). The dioritic and tonalitic rocks that form the western margin of the central gneisses, structurally overlying the western part of the Isua Greenstone Belt and its footwall, contain deformed Tarssartôq dykes, some of which are truncated at fault contacts (see above). These time markers imply that a component of the deformation in rocks structurally above the western Isua Greenstone Belt occurred after ~ 3.5 Ga, and is significantly younger than the formation of the underlying mylonitic panels. In contrast to the mylonitic panels, this younger deformation was apparently non-penetrative, with strong fabrics restricted to the base of the leucodiorite and along the structurally higher fault that truncates the Tarssartôq dykes (dykes 2 and 3 in Fig. 3). Although there is no outcrop-scale kinematic evidence, we speculate that this later deformation involved renewed thrusting, potentially to the northwest. The abrupt nature of the contacts between the mylonitic panels of the footwall and the local evidence for brittle faulting along some contacts, described above, suggests that renewed thrusting may have resulted in

minor reactivation of the mylonitic nappe stack after ~ 3.5 Ga. We suggest that this reactivation event is Neoarchean in age (Hanmer et al., submitted for publication).

8. Mylonitic thrust-nappe stack

Two end-member interpretations can be applied to the structure of the footwall to the western part of the Isua Greenstone Belt. The juxtaposition of panels of plutonic and supracrustal origin could represent an initial intrusive relationship that was subjected to penetrative mylonitisation in a coherent shear zone, at least ~ 1.5 km thick. In this scenario, the shear zone would have been reworked by three kinematically distinct events, but not significantly dislocated. The presence of amphibole as a fabric-forming mineral in the mafic schist, and the mixed brittle and crystal plastic behaviour of plagioclase in the tonalites, are compatible with the regional lower amphibolite facies metamorphic conditions (550 °C at 5 kbar) recorded by Boak and Dymek (1982) from the greenstone belt itself. Such thermal conditions are potentially compatible with active shearing throughout the thickness of the shear zone (e.g., Hanmer, 1988b; Hanmer et al., 1992). However, the following evidence suggests that finite displacements have occurred across the panel boundaries: (i) different tonalites occur on either side of the supracrustal panels, (ii) differences in penetrative strain state occur from one tonalite panel to the next, (iii) intrusive tonalite veins show a uniform distribution within supracrustal panels, unrelated to proximity to the bounding tonalite panels, (iv) there is no correspondence between the type of mafic inclusions in the tonalite panels and the adjacent supracrustal panels, and (v) lithological contacts at the panel boundaries are abrupt. The magnitude of such displacements is unconstrained, but would have to be sufficient to account for the lithological individuality of the abruptly juxtaposed panels.

Alternatively, in a second end-member scenario, transverse displacement vectors in a penetratively mylonitic homocline comprising panels of contrasting composition, associated with locally preserved evidence of strain gradients along the lower boundaries of the panels, could be interpreted in terms of a stack of penetratively mylonitic crystalline thrust-nappes (e.g., Hanmer, 1988a; Hanmer and McEachern, 1992; Nadeau and Hanmer, 1992). The fundamental difference between this scenario and the model of a dislocated shear zone would lie in the greater magnitude of the displacement across the nappe boundaries. Although systematic kinematic analysis has only been undertaken in the layered mylonite panels and the quartz–tremolite mylonites, the presence of pervasive mylonites and identical extension lineation patterns in the other footwall panels suggests that they can be similarly interpreted. For example, near the south end of Lake 704, we interpret the outlier of thickly banded amphibolite at the lake shore as a klippe (panel #10a in Fig. 3), isolated from the main nappe (panel #10) by erosion.

9. Modern structural regime in the Paleoarchean

Our observations suggest that the footwall to the western part of the Isua Greenstone Belt constitutes the oldest thrust-nappe stack known on Earth. However, the Paleoarchean deformation style and structural sequence are similar to those of modern mountain belts. During the middle Eocene, the Pennine nappes of the Western Alps were translated to the northwest by sinistral, strike-slip displacements (Ricou, 1984). By the late Oligocene–early Miocene, the displacement vector had progressively rotated ~ 90° anticlockwise as the deformation style evolved to southwest directed thrusting (Merle and Brun, 1984). Similarly, transverse contraction accommodated by the Basal Briançonnais Thrust, a composite structure of similar dimensions to the mylonitic footwall to the western Isua Greenstone Belt, postdates strike-parallel thrusting preserved in its hanging wall (Freeman et al., 1998). After the stacking of the nappes, the thickened Pennine crust underwent extensional shear along easterly dipping shear zones, commonly re-utilising the older contractional shear zones (Marquer et al., 1996). We emphasise that the comparison we make here refers only to the structural history; we have no constraints regarding the tectonic boundary conditions that drove the Paleoarchean deformation.

Historically, the role of continental crust in accommodating the higher global heat flow budget of the Archean Earth has been the subject of some debate.

For example, Bridgwater et al. (1974) speculated that high geothermal gradients in a hot early Earth would inhibit the formation of a thick continental crust. Other workers, however, found that continental crust shows no evidence for a higher temperature regime during the Archean (e.g., Sleep and Windley, 1982; England and Bickle, 1983). Our structural observations on the style and scale (see Hanmer and Greene, submitted for publication) of ~ 3.64 Ga deformation in the Isukasia area suggest that Paleoarchean continental crust responded to far-field shortening in a manner closely comparable with modern crust, leading us to conclude that its overall constitution, dimensions, thermal structure and rheology may not have been very different from those of continental crust today.

Acknowledgements

Thanks are extended to the Danish Natural Science Research Council, to the Commission for Scientific Research in Greenland and to the Minerals Office, Greenland Government, for generous support to the Isua Multidisciplinary Research Project (IMRP) to which this is a contribution. We are grateful to our international IMRP colleagues for sharing their observations and experience with us, in particular Peter Appel, Jim Crowley, John Myers, Ali Polat and Hugh Rollinson. Special thanks are due to Peter Appel for inviting us to work in the Isukasia area, and for his unflagging support of this study. Stereoplots were constructed and analysed using the freeware package "Stereonet", written and maintained by Rick Almendinger. We thank Wouter Bleeker, Sally Pehrsson, Cees van Staal, Jim Crowley, John Myers, and Journal reviewers, Bob Holdsworth and Vic McGregor for discussion, and/or careful, critical reviews. This is Geological Survey of Canada contribution #1999294.

References

Allaart, J.H., 1976a. The pre-3760 m.y. old supracrustal rocks of the Isua area, Central West Greenland, and the associated occurrence of quartz-banded ironstone. In: Windley, B.F. (Ed.), The Early History of the Earth. Wiley, London, pp. 177–189.

Allaart, J.H., 1976b. Continued mapping of the pre-3760 m.y. old supracrustal rocks of the Isua area, southern West Greenland. Rapport - Groenlands Geologiske Undersoegelse 80, 70–72.

Alsop, G.I., Holdsworth, R.E., 1999. Vergence and facing patterns in large-scale sheath folds. Journal of Structural Geology 21, 1335–1349.

Anthony, M., Wickham, J., 1978. Finite-element simulation of asymmetric folding. Tectonophysics 47, 1–14.

Appel, P.W.U., 1983. Tourmaline in the early Archaean Isua supracrustal belt, West Greenland. Journal of Geology 92, 599–605.

Appel, P.W.U., Fedo, C.M., Moorbath, S., Myers, J.S., 1998a. Early Archaean Isua supracrustal belt, West Greenland: pilot study of the Isua Multidisciplinary Research Project. Geology of Greenland Survey Bulletin 180, 94–99.

Appel, P.W.U., Fedo, C.M., Moorbath, S., Myers, J.S., 1998b. Recognizable primary volcanic and sedimentary features in a low strain domain of the highly deformed, oldest known (~ 3.7–3.8 Gyr) greenstone belt, Isua, West Greenland. Terra Nova 10, 57–62.

Bell, T.H., Hammond, R.L., 1984. On the internal geometry of mylonite zones. Journal of Geology 92, 667–686.

Boak, J.L., Dymek, R.F., 1982. Metamorphism of the ca. 3800 Ma supracrustal rocks at Isua, West Greenland: implications for early Archaean crustal evolution. Earth and Planetary Science Letters 59, 155–176.

Bridgwater, D., McGregor, V.R., 1974. Field work on the very early Precambrian rocks of the Isua area, southern West Greenland. Rapport - Groenlands Geologiske Undersoegelse 65, 49–54.

Bridgwater, D., McGregor, V.R., Myers, J.S., 1974. A horizontal tectonic regime in the Archaean of Greenland and its implications for early crustal thickening. Precambrian Research 1, 179–197.

Bridgwater, D., Keto, L., McGregor, V.R., Myers, J.S., 1976. Archaean gneiss complex of Greenland. In: Escher, A., Watt, W.S. (Eds.), Geology of Greenland. The Geological Survey of Greenland, Copenhagen, pp. 19–75.

Burke, K., Dewey, J.F., Kidd, W.S.F., 1976. Dominance of horizontal movements, arc and microcontinental collisions during the later permobile regime. In: Windley, B.F. (Ed.), The Early History of the Earth. Wiley, London, pp. 113–129.

Chadwick, B., Crewe, M.A., Park, J.F.W., 1983. Field work in the north of the Ivisârtoq region, inner Godthåbsfjord, southern West Greenland. Rapport - Groenlands Geologiske Undersoegelse 115, 49–56.

Chardon, D., Choukroune, P., Jayananda, M., 1998. Sinking of the Dharwar Basin (South India): implications for Archaean tectonics. Precambrian Research 91, 15–39.

Cobbold, P.R., Quinquis, H., 1980. Development of sheath folds in shear regimes. Journal of Structural Geology 2, 119–126.

Collins, W.J., van Kranendonk, M.J., Teyssier, C., 1998. Partial convective overturn of Archaean crust in the east Pilbara Craton, Western Australia: driving mechanisms and tectonic implications. Journal of Structural Geology 20, 1405–1424.

Crowley, J.L., Myers, J.S., Dunning, G.R., 2000. The timing and nature of 3700–3600 Ma magmatism, deformation and metamorphism north of the Isua Greenstone Belt, Greenland. American Geophysical Union, Program with Abstracts, H62C-10.

de Wit, M.J., 1998. On Archean granites, greenstones, cratons and

tectonics: does the evidence demand a verdict? Precambrian Research 91, 181–226.

de Wit, M.J., Armstrong, R., Hart, R.J., Wilson, A.H., 1987. Felsic igneous rocks within the 3.3 to 3.5 Ga Barberton Greenstone Belt: high crustal level equivalents of the surrounding tonalite–trondhjemite terrain, emplaced during thrusting. Tectonics 6, 529–549.

de Wit, M.J., Roering, C., Hart, R.J., Armstrong, R.A., de Ronde, C.E.J., Green, R.W.E., Tredoux, M., Peberdy, E., Hart, R.A., 1992. Formation of an Archean continent. Nature 357, 553–562.

Dymek, R.F., Boak, J.L., Kerr, M.T., 1983. Green micas in the Archaean Isua and Malene supracrustal rocks, southern West Greenland, and the occurrence of a barian–chromian muscovite. Rapport - Groenlands Geologiske Undersoegelse 112, 71082.

England, P., Bickle, M., 1983. Continental thermal and tectonic regimes during the Archaean. Journal of Geology 92, 353–367.

Fedo, C.M., 2000. Setting and origin for problematic rocks from the >3.7 Ga Isua Greenstone Belt, southern west Greenland: Earth's oldest coarse clastic sediment. Precambrian Research 101, 69–78.

Fitzgerald, J.D., Stunitz, H., 1993. Deformation of granitoids at low metamorphic grade: I. Reactions and grain size reduction. Tectonophysics 221, 269–297.

Freeman, S.R., Butler, R.W.H., Cliff, R.A., Inger, S., Barnicoat, A.C., 1998. Deformation migration in an orogen-scale shear zone array: an example from the Basal Briançonnais Thrust, internal Franco–Italian Alps. Geological Magazine 135, 349–367.

Frei, R., Bridgwater, D., Rosing, M., Stecher, O., 1999. Controversial Pb–Pb and Sm–Nd isotope results in the early Archean Isua (West Greenland) oxide iron formation: preservation of primary signatures versus secondary disturbances. Geochimica et Cosmochimica Acta 63, 473–488.

Friend, C.R.L., Nutman, A.P., Baadsgaard, H., Kinny, P.D., McGregor, V.R., 1996. Timing of late Archean assembly, crustal thickening and granite emplacement in the Nuuk region, southern West Greenland. Earth and Planetary Science Letters 142, 353–365.

Garde, A.A., 1997. Accretion and evolution of an Archaean high-grade grey gneiss–amphibolite complex: the Fiskefjord area, southern West Greenland. Geological Survey of Greenland, Bulletin 177, 115.

Garde, A.A., Larsen, O., Nutman, A.P., 1986. Dating of late Archean crustal mobilisation north of Qugssuk, Godthåbsfjord, southen West Greenland. Rapport - Groenlands Geologiske Undersoegelse 128, 23–36.

Ghosh, S.K., Mandal, N., Sengupta, S., Deb, S.K., Khan, D., 1993. Superposed buckling in multilayers. Journal of Structural Geology 15, 95–111.

Gill, R.C.O., Bridgwater, D., Allaart, J.H., 1981. The geochemistry of the earliest known basic metavolcanic rocks, at Isua, West Greenland: a preliminary investigation. Special Publication - Geological Society of Australia 7, 313–325.

Gruau, G., Rosing, M., Bridgwater, D., Gill, R.C.O., 1996. Resetting of Sm–Nd systematics during metamorphism of >3.7-Ga rocks: implications for isotopic models of early Earth differentiation. Chemical Geology 133, 225–240.

Hamilton, W.B., 1998. Archean magmatism and deformation were not products of plate tectonics. Precambrian Research 91, 143–179.

Hanmer, S., 1982. Microstructure and geochemistry of plagioclase and microcline in naturally deformed granite. Journal of Structural Geology 4, 197–213.

Hanmer, S., 1984. Strain-insensitive foliations in polymineralic rocks. Canadian Journal of Earth Sciences 21, 1410–1414.

Hanmer, S., 1988a. Ductile thrusting at mid-crustal level, southwestern Grenville Province. Canadian Journal of Earth Sciences 25, 1049–1059.

Hanmer, S., 1988b. Great Slave Lake Shear Zone, Canadian Shield: reconstructed vertical profile of a crustal-scale fault zone. Tectonophysics 149, 245–264.

Hanmer, S., McEachern, S.J., 1992. Kinematical and rheological evolution of a crustal-scale ductile thrust zone, Central Metasedimentary Belt, Grenville orogen. Canadian Journal of Earth Sciences 29, 1779–1790.

Hanmer, S., Passchier, C.W., 1991. Shear-sense indicators: a review. Geological Survey of Canada, Paper 90-17, 72 pp.

Hanmer, S., Greene, D.C., Is the Isua Greenstone Belt an early Archean (~ 3.64 Ga) crustal-scale sheath fold? Implications for early continental crust. Submitted to Geology.

Hanmer, S., Bowring, S., van Breemen, O., Parrish, R., 1992. Great Slave Lake shear zone, NW Canada: mylonitic record of Early Proterozoic continental convergence, collision and indentation. Journal of Structural Geology 14, 757–773.

Hanmer, S., Hamilton, M.A., Crowley, J.L., Geochronological constraints on Paleoarchean thrust-nappe and Neoarchean accretionary tectonics in southern West Greenland. Submitted to Tectonophysics.

Hansen, E., 1971. Strain facies. Minerals, Rocks and Inorganic Minerals. Springer-Verlag, New York, 192 pp.

James, P.R., 1976. Deformation of the Isua block, West Greenland: a remnant of the earliest stable continental crust. Canadian Journal of Earth Sciences 13, 816–823.

Komiya, T., Maruyama, S., Masuda, T., Nohda, S., Hayashi, M., Okamoto, K., 1999. Plate tetctonics at 3.8–3.7 Ga: field evidence from the Isua accretionary complex, southern West Greenland. Journal of Geology 107, 515–554.

Lin, S., Jiang, D., Williams, P.F., 1998. Transpression (or transtension) zones of triclinic symmetry: natural example and theoretical modelling. In: Holdsworth, R.E., Strachan, R.A., Dewey, J.F. (Eds.), Continental Transpressional and Transtensional Tectonics, Geological Society, Special Publication. Geological Society Special Publications. Geological Society, London, pp. 41–57.

Mackinnon, P., Fueten, F., Robin, P.Y., 1997. A fracture model for quartz ribbons in straight gneisses. Journal of Structural Geology 19, 1–14.

Manz, R., Wickham, J., 1978. Experimental analysis of folding in simple shear. Tectonophysics 44, 79–90.

Marquer, D., Challandes, N., Baudin, T., 1996. Shear zone patterns and strain distribution at the scale of a Penninic Nappe: the Suretta Nappe (Eastern Swiss Alps). Journal of Structural Geology 18, 753–764.

Marshak, S., 1999. Deformation style way back when: thoughts on

the contrasts between Archean/Paleoproterozoic and contemporary orogens. Journal of Structural Geology 21, 1175–1182.

Merle, O., Brun, J.P., 1984. The curved translation path of the Parpaillion Nappe (French Alps). Journal of Structural Geology 6, 711–719.

Moorbath, S., O'Nions, R.K., Pankhurst, R.J., 1973. Early Archaean age for the Isua Iron Formation, West Greenland. Nature 245, 138–139.

Nadeau, L., Hanmer, S., 1992. Deep-crustal break-back stacking and slow exhumation of the continental footwall beneath a thrusted marginal basin, Grenville Orogen, Canada. Tectonophysics 210, 215–233.

Nutman, A.P., 1982. Further work on the early Archaean rocks of the Isukasia area, southern West Greenland. Rapport - Groenlands Geologiske Undersoegelse 110, 49–54.

Nutman, A.P., 1984. Early Archaean crustal evolution of the Isukasia area, southern West Greenland. In: Kroner, A., Greiling, R. (Eds.), Precambrian Tectonics Illustrated. E. Schweizerbart'sche Verlagsbuchhandlung, Stuttgart, pp. 79–93.

Nutman, A.P., 1986. The early Archaean to Proterozoic history of the Isukasia area, southern West Greenland. Groenlands Geologiske Undersoegelse, Bulletin 154, 80.

Nutman, A.P., Bridgwater, D., 1986. Early Archaean Amîtsoq tonalites and granites of the Isukasia area, southern West Greenland: development of the oldest-known sial. Contributions to Mineralogy and Petrology 94, 137–148.

Nutman, A.P., Allaart, J.H., Bridgwater, D., Dimroth, E., Rosing, M., 1984. Stratigraphic and geochemical evidence for the depositional environment of the early Archaean Isua supracrustal belt, southern West Greenland. Precambrian Research 25, 365–396.

Nutman, A.P., Friend, C.R.L., Baadsgaard, H., McGregor, V.C., 1989. Evolution and assembly of Archean gneiss terranes in the Godthabsfjord region, southern West Greenland: structural, metamorphic and isotopic evidence. Tectonics 8, 573–589.

Nutman, A.P., Friend, C.R.L., Kinny, P.D., McGregor, V.R., 1993. Anatomy of an Early Archean gneiss complex: 3900–3600 crustal evolution in southern West Greenland. Geology 21, 415–418.

Nutman, A.P., McGregor, V.R., Friend, C.R.L., Bennett, V.C., Kinny, P.D., 1996. The Itsaq Gneiss Complex of southern West Greenland; the world's most extensive record of early crustal evolution (3900–3600 Ma). Precambrian Research 78, 1–39.

Nutman, A.P., Bennett, V.C., Friend, C.R.L., Rosing, M.T., 1997. $\sim$ 3710 and $\geq$ 3790 Ma volcanic sequences in the Isua (Greenland) supracrustal belt; structural and Nd isotope implications. Chemical Geology 141, 271–287.

Nutman, A.P., Bennett, V.C., Friend, C.R.L., Norman, M.D., 1999. Meta-igneous (non-gneissic) tonalites and quartz–diorites from an extensive ca. 3800 Ma terrain south of the Isua supracrustal belt, southern West Greenland: constraints on early crust formation. Contributions to Mineralogy and Petrology 137, 364–388.

Nutman, A.P., Bennett, V.C., Friend, C.R.L., McGregor, V.R., 2000. The early Archaean Itsaq Gneiss Complex of southern West Greenland: the importance of field observations in interpreting age and isotopic constraints for early terrestrial evolution. Geochimica et Cosmochimica Acta 64, 3035–3060.

O'Hara, K.D., 1994. Fluid–rock interaction in crustal shear zones: a directed percolation approach. Geology 22, 843–846.

Park, R.G., 1997. Early Precambrian plate tectonics. South African Journal of Geology 100, 23–35.

Passchier, C.W., 1998. Monoclinic model shear zones. Journal of Structural Geology 20, 1121–1137.

Passchier, C.W., den Brok, S.W.J., van Gool, J.A.M., Marker, M., Manatschal, G., 1997. A laterally constricted shear zone system—the Nordre Stromfjord steep belt, Nagssugtoqidian Orogen, W. Greenland. Terra Nova 9, 199–202.

Pryer, L.L., 1993. Microstructures in feldspars from a major crustal thrust zone: the Grenville Front, Ontario, Canada. Journal of Structural Geology 15, 21–36.

Ranalli, G., Murphy, D.C., 1987. Rheological stratification of the lithosphere. Tectonophysics 132, 281–295.

Ricou, L.E., 1984. Les Alpes Occidentales: chaine de décrochement. Bulletin de la Societe Geologique de France 26, 861–874.

Rosing, M.T., Rose, N.M., Bridgwater, D., Thomsen, H.S., 1996. Earliest part of Earth's stratigraphic record: a reappraisal of the >3.7 Ga Isua (Greenland) supracrustal sequence. Geology 24, 43–46.

Rutter, E.H., Brodie, K.H., 1988. The role of tectonic grain size reduction in the rheological stratification of the lithosphere. Geologische Rundschau 77, 295–308.

Rutter, E.H., Brodie, K.H., 1991. Lithosphere rheology—a note of caution. Journal of Structural Geology 13, 363–367.

Rutter, E.H., Brodie, K.H., 1992. Rheology of the lower crust. In: Fountain, D.M., Arculus, R.J., Kay, R.W. (Eds.), Continental Lower Crust. Elsevier, Amsterdam, pp. 201–267.

Sleep, N.H., Windley, B.F., 1982. Archean plate tectonics: constrain and inferences. Journal of Geology 90, 363–379.

Smith, G.M., Dymek, R.F., 1983. A description and interpretation of the Proterozoic Kobbefjord Fault Zone, Godthab district, West Greenland. Rapport - Groenlands Geologiske Undersoegelse 112, 113–127.

White, R.V., Crowley, J.L., Parrish, R., David, K., 2000. Gate-crashing the billionth birthday party: intrusion of dyke swarms in the Isua region. American Geophysical Union, Program with Abstracts, V51D–05.

Whitehouse, M.J., Kamber, B.S., Moorbath, S., 1999. Age significance of U–Th–Pb zircon data from early Archaean rocks of west Greenland—a reassessment based on combined ion-microscope and imaging studies. Chemical Geology 160, 201–224.